

Structures of TMC-95A–D: Novel Proteasome Inhibitors from *Apiospora montagnei* Sacc. TC 1093

Jun Kohno,* Yutaka Koguchi, Maki Nishio, Kazuya Nakao, Masataka Kuroda, Ryo Shimizu, Tetsuo Ohnuki, and Saburo Komatsubara

Discovery Research Laboratory, Tanabe Seiyaku Co., Ltd., 2-50 Kawagishi-2-chome, Toda-shi, Saitama 335-8505, Japan

Received August 31, 1999

Four novel proteasome inhibitors, TMC-95A–D (**1–4**) have been isolated from the fermentation broth of *Apiospora montagnei* Sacc. TC 1093, isolated from a soil sample. All of the molecular formulas of **1–4** were established as $C_{33}H_{38}N_6O_{10}$ by high-resolution FAB-MS. Their planar structures were determined on the basis of extensive analyses of 1D and 2D NMR, and degradation studies. Compounds **1–4** have the same planar structures to each other, and are unique highly modified cyclic peptides containing L-tyrosine, L-asparagine, highly oxidized L-tryptophan, (*Z*)-1-propenylamine, and 3-methyl-2-oxopentanoic acid units. The absolute configuration at C-11 and C-36 of **1–4** was determined based on chiral TLC and HPLC analyses of their chemical degradation products. The ROESY analysis along with 1H - 1H coupling constants clarified the absolute stereochemistry at C-6, -7, -8, and -14 of the cyclic moieties. These studies revealed the relationships of **1–4** to be diastereomers at C-7 and C-36.

Introduction

Proteasomal proteolysis is a major extralysosomal proteolytic system in eucaryotes. The catalytic core of the proteasome is the 20S proteasome, which is a large cylindrically shaped complex composed of a stack of four rings, each containing seven subunits, $\alpha_7\beta_7\beta_7\alpha_7$.¹ The 20S proteasome has N-terminal threonine residues of the β -subunits as its active sites, and it shows at least three distinct peptidase activities: chymotrypsin-like, trypsin-like, and peptidylglutamyl-peptide hydrolyzing activities.^{1,2}

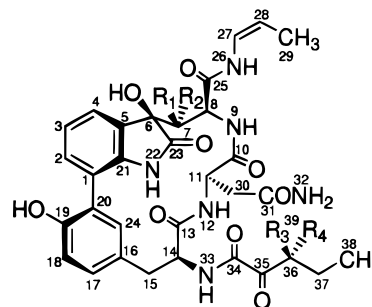
Recently, proteasomal proteolysis has been shown to play critical roles in the activation of NF- κ B, which has been observed in a variety of inflammatory diseases,³ as well as the processing of histocompatibility complex. Inhibitors of the 20S proteasome thus might be useful for the treatment of inflammatory and autoimmune diseases.

In the course of our screening program for proteasome inhibitors, TMC-95A–D (**1–4**) have been isolated from the fermentation broth of *Apiospora montagnei* Sacc. TC 1093, isolated from a soil sample. These compounds are structurally characterized by novel and unique cyclic peptides. In this paper, we report the structure determination of TMC-95A–D. The taxonomy, fermentation, isolation, and biological activities will be reported in a separate paper.⁴

Results

TMC-95A–D (**1–4**) have similarities in most of physicochemical properties as follows. All of the molecular

formulas of **1–4** were determined to be $C_{33}H_{38}N_6O_{10}$ by HRFAB-MS [(M + H)⁺: found *m/z* **1**: 679.2728, **2**: 679.2747, **3**: 679.2729, and **4**: 679.2744; calcd *m/z* 679.2728]. The IR spectra of the all compounds indicated the presence of hydroxyl (3400–3380 cm^{-1}), carbonyl (1720 cm^{-1}), and amide (1660 and 1515–1510 cm^{-1}) groups. These compounds showed UV absorption maxima at 294–301 nm in MeOH, which were shifted to 303–304 nm (**1** and **3**) or 312–313 nm (**2** and **4**) in alkaline solution. They differed in their specific optical rotation values ([α]_D, **1**: +102°, **2**: +74°, **3**: -18°, and **4**: -36°), however. These results suggested that TMC-95A–D (**1–4**) were peptides containing the chromophore, and were diastereomers to each other.



TMC-95	R ₁	R ₂	R ₃	R ₄
A (1)	H	OH	CH ₃	H
B (2)	H	OH	H	CH ₃
C (3)	OH	H	CH ₃	H
D (4)	OH	H	H	CH ₃

TMC-95A (1). The ^{13}C (100 MHz) and 1H NMR (400 MHz) data in DMSO-*d*₆ at 30 °C are shown in Tables 1 and 2, respectively. The ^{13}C NMR spectrum of **1** displayed 33 signals composed of 3 methyl carbons, 3 methylene carbons, 13 methine carbons including 8 olefinic and 3

* To whom correspondence should be addressed. Tel.: +81-48-433-2732. Fax: +81-48-433-2734. E-mail: jun-k@tanabe.co.jp.

(1) Ciechanover, A.; Schwartz, A. L. *Proc. Natl. Acad. Sci. U.S.A.* **1998**, *95*, 2727–2730.

(2) Orlowski, M.; Michaud, C. *Biochemistry* **1989**, *28*, 9270–9278.

(3) Palombella, V. J.; Rando, O. J.; Goldberg, A. L.; Maniatis, T. *Cell* **1994**, *78*, 773–785.

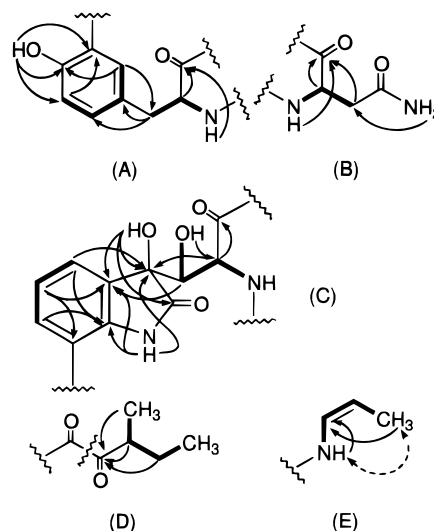
(4) Koguchi, Y.; Kohno, J.; Nishio, M.; Takahashi, K.; Okuda, T.; Ohnuki, T.; Komatsubara, S. *J. Antibiot.* **2000**, *53* (2), in press.

Table 1. ^{13}C NMR Data for TMC-95A (1), -B (2), -C (3), and -D (4)

no.	1	2	3	4
1	120.4 s	120.4 s	120.6 s	120.6 s
2	130.7 d	130.7 d	131.0 d	131.0 d
3	120.4 d	120.4 d	120.8 d	120.8 d
4	124.9 d	124.9 d	121.8 d	121.8 d
5	129.1 s	129.1 s	129.9 s	129.9 s
6	77.5 s	77.5 s	76.3 s	76.3 s
7	75.2 d	75.2 d	76.5 d	76.5 d
8	54.4 d	54.4 d	53.7 d	53.7 d
10	170.3 s	170.3 s	171.6 s	171.6 s
11	49.5 d	49.5 d	49.4 d	49.4 d
13	170.1 s	170.1 s	170.1 s	170.1 s
14	51.6 d	51.5 d	51.5 d	51.5 d
15	36.5 t	36.6 t	36.4 t	36.5 t
16	125.0 s	125.0 s	125.0 s	125.0 s
17	129.8 d	129.9 d	130.0 d	130.1 d
18	115.0 d	115.1 d	115.1 d	115.1 d
19	153.1 s	153.1 s	153.1 s	153.1 s
20	122.9 s	122.9 s	122.7 s	122.7 s
21	139.9 s	139.9 s	139.7 s	139.7 s
23	177.9 s	177.9 s	177.0 s	177.0 s
24	132.9 d	133.0 d	132.6 d	132.7 d
25	167.2 s	167.2 s	168.3 s	168.3 s
27	122.3 d	122.3 d	121.8 d	121.8 d
28	105.0 d	105.0 d	106.4 d	106.4 d
29	11.2 q	11.2 q ^a	11.0 q	11.0 q ^b
30	36.6 t	36.6 t	36.4 t	36.5 t
31	170.1 s	170.1 s	170.5 s	170.5 s
34	158.8 s	158.9 s	158.9 s	159.0 s
35	201.3 s	201.3 s	201.3 s	201.3 s
36	39.5 d	40.0 d	39.5 d	40.0 d
37	24.8 t	24.5 t	24.8 t	24.5 t
38	11.0 q	11.1 q ^a	11.0 q	11.1 q ^b
39	14.5 q	14.7 q	14.4 q	14.7 q

^{a,b} May be exchangeable.

α -methine carbons, 7 quaternaries including 6 olefinic carbons, and 7 carbonyl carbons including 6 amide and an ketone carbons. The ^1H NMR spectrum of **1** showed the presence of seven amide protons (δ 6.95, 7.23, 7.28,

**Figure 1.** DQF-COSY, HMBC, and ROESY correlations of the partial structures A–E. Bold lines show proton spin systems, arrows indicate HMBC correlations, and a dashed line indicates ROESY correlation.

8.10, 8.20, 9.00, and 9.01) and three hydroxyl protons (δ 5.77, 6.18, and 9.35). The extensive 2D-NMR experiments including COSY, pulsed field gradient (pfg)-HMBC, and ROESY (rotating frame nuclear Overhauser effect spectroscopy) revealed the presence of five partial structures (A–E) (Figure 1).

The partial structure A was established to be a *meta*-substituted tyrosine based on HMBC correlations H-14 (δ 4.66)/C-13 (δ 170.1), H-15 (δ 3.07 and 2.95)/C-16 and C-17, H-24/C-15 (δ 36.5), H-18/C-20, and OH-19 (δ 9.35)/C-18 (δ 115.0), C-19 (δ 153.1) and C-20 (δ 122.9). In the partial structure B, the presence of an asparagine unit was deduced from HMBC correlations NH₂-32 (δ 7.28 br s and

Table 2. ^1H NMR Data for TMC-95A (1), -B (2), -C (3) and -D (4)

no.	1	2	3	4
2	7.24 (1H, dd, 1, 7.5)	7.24 (1H, dd, 0.9, 7.5)	7.26 (1H, d, 7.6)	7.26 (1H, d, 7.6)
3	6.97 (1H, t, 7.5)	6.97 (1H, t, 7.5)	7.02 (1H, t, 7.6)	7.02 (1H, t, 7.6)
4	7.35 (1H, dd, 1, 7.5)	7.35 (1H, dd, 0.9, 7.5)	7.19 (1H, d, 7.6)	7.19 (1H, d, 7.6)
7	4.17 (1H, dd, 4.4, 10.7)	4.17 (1H, dd, 4.4., 10.7)	4.34 (1H, d, 4)	4.34 (1H, d, 4)
8	3.92 (1H, t, 10)	3.92 (1H, t, 10)	4.01 (1H, d, 9.5)	4.01 (1H, d, 9.4)
11	4.64 (1H, m)	4.64 (1H, m)	4.66 (1H, m)	4.66 (1H, m)
14	4.66 (1H, m)	4.66 (1H, m)	4.68 (1H, m)	4.68 (1H, m)
15a	2.95 (1H, dd, 4.8, 13.6)	2.93 (1H, dd, 4.8, 13.7)	2.95 (1H, dd, 5.0, 13.8)	2.94 (1H, dd, 5.0, 13.5)
15b	3.07 (1H, dd, ~2, 13.6)	3.07 (1H, dd, ~2, 13.7)	3.09 (1H, dd, ~2, 13.8)	3.09 (1H, brd, 13.5)
17	6.66 (1H, dd, 2.2, 8.1)	6.70 (1H, dd, 2.2, 8.1)	6.68 (1H, dd, 2.2, 8.1)	6.72 (1H, dd, 2.0, 8.1)
18	6.77 (1H, d, 8.1)	6.79 (1H, d, 8.1)	6.78 (1H, d, 8.1)	6.80 (1H, d, 8.1)
24	7.17 (1H, d, 2.2)	7.17 (1H, d, 2.2)	7.09 (1H, d, 2.2)	7.09 (1H, d, 2)
27	6.46 (1H, qt, 1.7, 10)	6.46 (1H, qt, 1.7, 10)	6.46 (1H, qt, 1.7, 10)	6.46 (1H, qt, 1.7, 10)
28	4.66 (1H, m)	4.66 (1H, m)	4.76 (1H, m)	4.76 (1H, m)
29	1.60 (3H, dd, 1.7, 7.0)	1.60 (3H, dd, 1.7, 7.0)	1.60 (3H, dd, 1.7, 7.1)	1.60 (3H, dd, 1.5, 7.1)
30a	2.38 (1H, dd, 11.0, 15.9)	2.38 (1H, dd, 10.8, 15.7)	2.49 (1H, m)	2.49 (1H, m)
30b	2.45 (1H, dd, 3.6, 15.9)	2.45 (1H, dd, 3.6, 15.7)	2.85 (1H, dd, 3.4, 15.6)	2.85 (1H, dd, 3.3, 15.5)
36	3.38 (1H, m)	3.34 (1H, m)	3.38 (1H, m)	3.34 (1H, m)
37a	1.44 (1H, m)	1.35 (1H, m)	1.44 (1H, m)	1.35 (1H, m)
37b	1.69 (1H, m)	1.65 (1H, m)	1.69 (1H, m)	1.65 (1H, m)
38	0.87 (3H, t, 7.4)	0.82 (3H, t, 7.4)	0.87 (3H, t, 7.4)	0.82 (3H, t, 7.4)
39	1.01 (3H, d, 6.8)	1.07 (3H, d, 7.0)	1.01 (3H, d, 7.1)	1.07 (3H, d, 7.1)
9-NH	8.20 (1H, d, 9.8)	8.20 (1H, d, 9.8)	8.20 (1H, d, 9.5)	8.19 (1H, d, 9.4)
12-NH	9.01 (1H, d, 7.5)	9.01 (1H, d, 7.3)	9.06 (1H, d, 7.6)	9.05 (1H, d, 7.6)
22-NH	8.10 (1H, s)	8.10 (1H, s)	8.14 (1H, s)	8.14 (1H, s)
26-NH	9.00 (1H, d, 10.3)	9.01 (1H, d, 10.8)	8.60 (1H, d, 10.3)	8.60 (1H, d, 10.3)
32-NH ₂	7.28, 6.95 (2H, brs)	7.29, 6.95 (2H, brs)	7.37, 7.00 (2H, brs)	7.37, 7.00 (2H, brs)
33-NH	7.23 (1H, d, 7.8)	7.23 (1H, d, 8.1)	7.24 (1H, d, 8)	7.24 (1H, d, 7.8)
6-OH	6.18 (1H, s)	6.18 (1H, s)	6.25 (1H, s)	6.24 (1H, s)
7-OH	5.77 (1H, d, 4.6)	5.77 (1H, d, 4.4)	5.64 (1H, d, 4)	5.64 (1H, d, 4)
19-OH	9.35 (1H, s)	9.35 (1H, s)	9.38 (1H, s)	9.38 (1H, s)

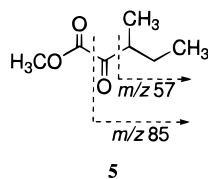


Figure 2. GC-EIMS fragmentations of **5**.

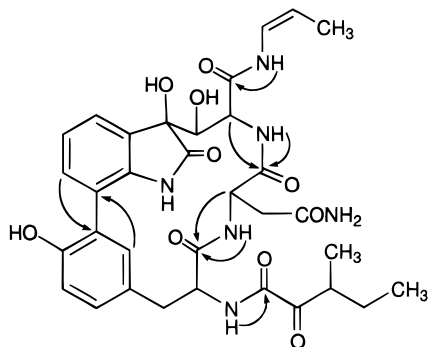


Figure 3. HMBC network of **1**, establishing the connectivity of the partial structures A–E.

6.95 br s)/C-30 (δ 36.6), and H-11 (δ 4.64)/C-10 (δ 170.3), and confirmed by TLC analysis of the acid hydrolysate of **1**, which gave an aspartic acid. In the partial structure C, the presence of 3-hydroxy-2-indolinone subunit was accomplished based on the HMBC data (NH-22 (δ 8.10)/C-21, C-5 and C-6 (δ 77.5), H-2 and H-4/C-21, H-3/C-5 and C-1, and OH-6 (δ 6.18)/C-6 and C-23 (δ 177.9)). In addition, HMBC correlations H-8 (δ 3.92)/C-25 (δ 167.2) and C-6, and H-7 (δ 4.17)/C-5 were observed. The partial structure C was thus determined as shown. 3-Methyl-2-oxopentanoate unit of D was confirmed by GC-EIMS analysis of the ethereal extract of the hydrolysate of **1**. The ethereal extract of the hydrolysate was treated with diazomethane to give the methyl ester derivative **5** of a fatty acid. The EIMS spectrum of **5** showed a molecular ion peak at m/z 144 along with two fragment ion peaks at m/z 85 and 57 (Figure 2). This observation was in good agreement with that of methyl 3-methyl-2-oxopentanoate in the literature.⁵ The partial structure E was determined to be a (*Z*)-1-propenylamine based on the proton spin systems and ROESY correlation H-29/NH-26, with coupling constant $^3J_{H-27,H-28} = 10$ Hz. The structure of α,β -unsaturated amine was supported by the observation of upfield chemical shift of the β -olefinic proton H-28 (δ 4.66) relative to the α proton H-27 (δ 6.46).⁶

The connectivities of these partial structures (A–E) were established by HMBC correlations of **1** as illustrated in Figure 3. Four amide protons (NH-9: δ 8.20, NH-12: δ 9.01, NH-26: δ 9.00, and NH-33: δ 7.23) showed two-bond correlations with adjacent amide carbons (C-10: δ 170.3, C-13: δ 170.1, C-25: δ 167.2, and C-34: δ 158.8). Also two aromatic protons H-2 (δ 7.24) and H-24 (δ 7.17) displayed three-bond correlations with C-20 (δ 122.9) and C-1 (δ 120.4), respectively. On the basis of the results of the NMR studies described above, the planar structure of TMC-95 A was determined to be a novel and unique peptide as shown.

The absolute stereochemistry of the cyclic moieties of **1** was determined by analyses of ROESY correlations,

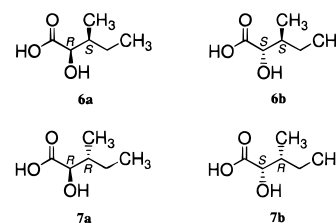
proton–proton coupling constants, and degradation studies as follows. Complete acid hydrolysis (6 N HCl, 115 °C, 15 h) of **1** gave L-aspartic acid which was identified by chiral TLC with authentic sample, showing the *S* configuration at C-11 of the asparagine residue.

The cyclic skeleton of **1** (C-1 to C-24) with *S* configuration at C-11 gave two highly rigid molecular models of atropisomers based on the stereochemistry at C-6. Between them the only model with *S* configuration at C-6 was consistent with the observation of ROESY correlation NH-22/H-11. The γ -lactam ring of the indolinone moiety oriented upward, and benzylic methylene group (C-15) of the tyrosine moiety downward as shown in Figure 4.

In the partial structure **a**, large coupling constants, $^3J_{NH-12,H-11} = 7.5$ Hz and $^3J_{H-30a,H-11} = 11.0$ Hz, coupled with ROESY correlation NH-12/H-30a suggested the trans geometry of the dihedral angle between H-11 and NH-12, and H-11 and H-30a. A small coupling constant $^3J_{H-30b,H-11} = 3.6$ Hz, along with ROESY correlations NH-9/H-11 and NH-9/H-30b indicated that NH-9, H-11, and H-30b protons were on the same side of the molecule. In the partial structure **b**, ROESY correlations H-14/NH-12 and NH-33/H-17 were observed. In addition, the small vicinal coupling constants of H-14 to H-15a and H-15b ($^3J_{H-14,H-15a} = 4.8$ Hz and $^3J_{H-14,H-15b} = 2$ Hz) and ROESY correlations H-14/H-15a and H-14/H-15b confirmed that H-14 proton should be located between H-15a and H-15b. The absolute configuration at C-14 was thus determined to be *S*.

In the partial structure **c**, a large coupling constant $^3J_{NH-9,H-8} = 9.8$ Hz and ROESY correlation NH-26/NH-9 indicated the trans geometry of the dihedral angle between NH-9 and H-8. The configuration at C-8 was thus assigned to be *S*. The observed large coupling constant $^3J_{H-7,H-8} = 10.7$ Hz and ROESY correlations H-7/NH-9, OH-7/H-8 and OH-7/H-4 indicated the trans geometry of the dihedral angle between H-8 and H-7, leading the configuration at C-7 to be *R*.

Stereochemistry of C-36 was determined by the degradation studies of **1**. Sodium borohydride reduction followed by acid hydrolysis (6 N HCl, 110 °C) of **1** yielded the mixture of *D*-*allo*-2-hydroxy-3-methylvaleric acid (**6a**) and *L*-2-hydroxy-3-methylvaleric acid (**6b**) on the basis of HPLC analysis using chiral column. The absolute configuration at C-36 was thus assigned to be *S*.



TMC-95B (2). The ^{13}C and ^1H NMR data of cyclic moiety in **2** were almost identical with those of **1** (^{13}C : $\delta_1 - \delta_2 = 0.0$ to -0.1 , ^1H : $\delta_1 - \delta_2 = 0.00$ except for H-15, 17, and 18). On the other hand, the prominent differences of the ^1H NMR chemical shifts between **1** and **2** were observed in the partial structure D. Proton signals of H-36 (δ 3.34), H-37 (δ 1.65 and 1.35), and H-38 (δ 0.82) in **2** were shifted to higher field, and H-39 (δ 1.07) was shifted to lower field relative to those of **1** (H-36: δ 3.38, H-37: δ 1.69 and 1.44, H-38: δ 0.87, and H-39: δ 1.01).

(5) Carlier, J.-P.; Sellier, N. *J. Chromatogr.* **1989**, *493*, 257–273.

(6) Stille, J. K.; Becker, Y. *J. Org. Chem.* **1980**, *45*, 2139–2145.

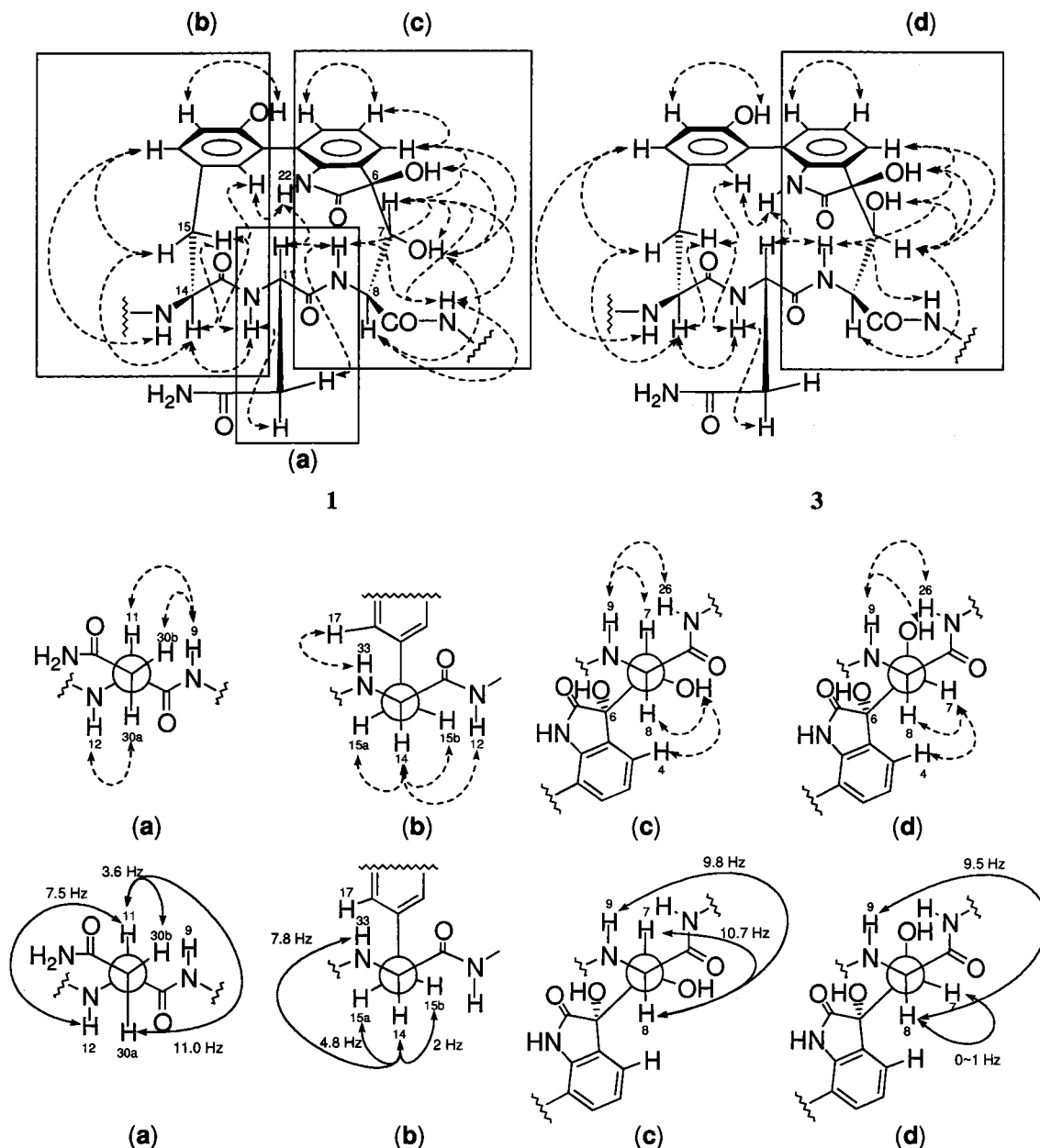


Figure 4. ROESY correlations and proton–proton coupling constants of **1** and **3**. Dashed arrows indicate ROESY correlations and arrows show proton–proton coupling constants.

The above results, together with the difference of the optical rotation values between **1** and **2**, demonstrated that TMC-95B (**2**) was the epimer at C-36 of **1**. Sodium borohydride reduction followed by acid hydrolysis of **2** indeed yielded the mixture of D-2-hydroxy-3-methylvaleric acid (**7a**) and L-*allo*-2-hydroxy-3-methylvaleric acid (**7b**). The absolute configuration of C-36 was thus assigned to be *R*.

TMC-95C (3). The ^{13}C and ^1H NMR data of **3** were slightly different in the cyclic moiety, and identical in the partial structure D, with those of **1**. Comparison and extensive analysis of DQF-COSY, pgf-HMQC, and pgf-HMBC suggested that **3** and **1** had the identical planar structure. The ROESY and proton–proton coupling data in **3** were almost identical with those in **1** except for the coupling constant of H-7 and ROESY correlations of H-7 and OH-7 in the partial structure **d** (see Table 2 and Figure 4). A very small coupling constant $^3J_{\text{H-7,H-8}} = 0\text{--}1$ Hz and ROESY correlations OH-7/NH-9, H-7/H-8, and

H-7/H-4 indicated the configuration at C-7 of **3** to be *S*. TMC-95C (**3**) was thus an epimer at C-7 of **1**.

TMC-95D (4). The ^{13}C and ^1H NMR data of **4** were identical with those of **3** except for the signals of the partial structure D. The signals corresponding (D) in **4** were identical with those in **2**. Consequently, TMC-95D (**4**) was determined to be an epimer at C-7 of **3**.

Molecular Modeling of 1 and 3. To investigate the three-dimensional structure of TMC-95A (**1**) and -C (**3**), we performed molecular modeling of these compounds. The initial coordinates were constructed by using SYBYL molecular modeling software. Conformational analyses were done by using Random Search option and Tripos force field of SYBYL. The twelve carbon–carbon or carbon–nitrogen bonds C-6/C-7, C-7/C-8, C-8/N-9, N-9/C-10, C-10/C-11, C-11/N-12, N-12/C-13, C-13/C-14, C-14/C-15, C-15/C-16, C-1/C-20, and C-11/C-30 were allowed to rotate during 2000 cycles of conformational searching. The resultant structures were exported to QUANTA

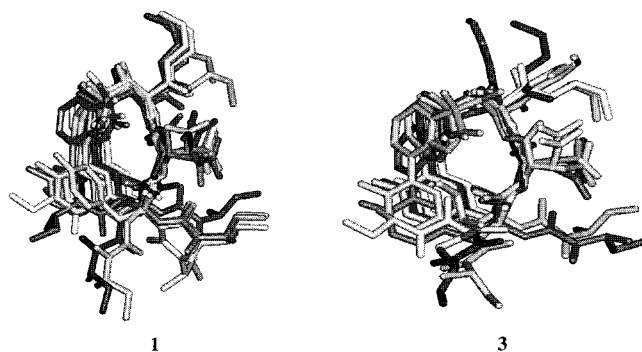


Figure 5. Superposition of stable conformers of **1** and **3** obtained from a conformational search.

molecular graphics software and energetically minimized by CHARMM force field. Distance-dependent dielectric constant was used to approximate the solvent effect. All structures obtained by CHARMM minimization coincided with the experimental results observed by NOEs that the distances between NH-22 and H-11 and NH-22 and H-24 were less than 5 Å. On the basis of superposition of **1** and **3**, there were three conformational families for both compounds as shown in Figure 5.

In this study, we discovered four new proteasome inhibitors, TMC-95A–D (**1**–**4**), from the fermentation broth of *Apiospora montagnei* Sacc. TC 1093. Our structural study characterized **1**–**4** to be novel cyclic peptides containing L-tyrosine, L-asparagine, highly oxidized L-tryptophan, (*Z*)-1-propenylamine, and 3-methyl-2-oxopentanoic acid units. The relationships of **1**–**4** was stereoisomers at C-7 and C-36 position.

The cyclic peptide cores of TMC-95s are structurally related to the partial structures of chlorinated hexapeptides such as complestatin,^{7,8} kistamycins,⁹ and chloropeptins.¹⁰ TMC-95s have 3-hydroxy-2-indolinone nucleus which coupled with tyrosine instead of indole nucleus connected with (*p*-hydroxyphenyl)glycine in the chlorinated hexapeptides.

TMC-95s have an α -keto group in the 3-methyl-2-oxopentanoic acid moiety. There are some serine protease inhibitors having the α -keto group, e.g., eurystatin A and B,¹¹ poststatin,¹² cyclotheonamides,¹³ and keramamides.¹⁴ The keto moiety in eurystatin A and B, and poststatin has been identified as the key functional group for the enzyme inhibitory activity.

Experimental Section

General Experimental Procedures. R_f values were determined with Kieselgel 60 F₂₅₄ TLC glass plates (E. Merck,

(7) Kaneko, K.; Kamoshida, K.; Takahashi, S. *J. Antibiot.* **1989**, *42*, 236–241.

(8) Seto, H.; Fujioka, T.; Furihata, K.; Kaneko, I.; Takahashi, S. *Tetrahedron Lett.* **1989**, *30*, 4987–4990.

(9) Naruse, N.; Oka, M.; Konishi, M.; Oki, T. *J. Antibiot.* **1993**, *46*, 1812–1818.

(10) Matsuzaki, K.; Ikeda, H.; Ogino, T.; Matsumoto, A.; Woodruff, H. B.; Tanaka, H.; Omura, S. *J. Antibiot.* **1994**, *47*, 1173–1174.

(11) Toda, S.; Kotake, C.; Tsuno, T.; Narita, Y.; Yamasaki, T.; Konishi, M. *J. Antibiot.* **1992**, *45*, 1580–1586.

(12) Nagai, M.; Ogawa, K.; Muraoka, Y.; Naganawa, H.; Aoyagi, T.; Takeuchi, T. *J. Antibiot.* **1991**, *44*, 956–961.

(13) Fusetani, N.; Matsunaga, S.; Matsumoto, H.; Takebayashi, Y. *J. Am. Chem. Soc.* **1990**, *112*, 7053–7054.

(14) Kobayashi, J.; Itagaki, F.; Shigemori, H.; Ishibashi, M.; Takahashi, K.; Ogura, M.; Nagasawa, S.; Nakamura, T.; Hirota, H.; Ohta, T.; Nozoe, S. *J. Am. Chem. Soc.* **1991**, *113*, 7812–7813.

Darmstadt, Germany) in CH₂Cl₂/MeOH (5:1). TLC spots were visualized by exposure to an ammonium molybdate/H₂SO₄ spray reagent.

TMC-95 A (1): colorless powder; $[\alpha]_D^{23} +102^\circ$ (*c* 0.54, MeOH); R_f value 0.36; UV (MeOH) λ_{\max} 206 (log ϵ 4.59), 222 (4.63), and 294 (3.74) nm, UV (0.1 N HCl–MeOH) λ_{\max} 204 (log ϵ 4.60), 222 (4.63), and 294 (3.74) nm, UV (0.1 N NaOH–MeOH) λ_{\max} 231 (log ϵ 4.62), 304 (3.91), and 374 (3.18) nm; IR (KBr) ν_{\max} 3380, 1720, 1660, and 1515 cm⁻¹; FAB-MS m/z 679 ($M + H$)⁺; HRFAB-MS m/z 679.2728 ($M + H$)⁺, (calcd for C₃₃H₃₉N₆O₁₀ 679.2728). The ¹H and ¹³C NMR data are given in Tables 1 and 2.

TMC-95 B (2): colorless powder; $[\alpha]_D^{23} +74^\circ$ (*c* 0.47, MeOH); R_f value 0.36; UV (MeOH) λ_{\max} 206 (log ϵ 4.60), 222 (4.62), and 295 (3.73) nm, UV (0.1 N HCl–MeOH) λ_{\max} 205 (log ϵ 4.62), 221 (4.62), and 295 (3.73) nm, UV (0.1 N NaOH–MeOH) λ_{\max} 230 (log ϵ 4.62) and 313 (3.81) nm; IR (KBr) ν_{\max} 3380, 1720, 1660, and 1515 cm⁻¹; FAB-MS m/z 679 ($M + H$)⁺; HRFAB-MS m/z 679.2747 ($M + H$)⁺, (calcd for C₃₃H₃₉N₆O₁₀ 679.2728). The ¹H and ¹³C NMR data are given in Tables 1 and 2.

TMC-95 C (3): colorless powder; $[\alpha]_D^{23} -18^\circ$ (*c* 0.23, MeOH); R_f value 0.12; UV (MeOH) λ_{\max} 207 (log ϵ 4.55), 222 (4.60), and 295 (3.72) nm, UV (0.1 N HCl–MeOH) λ_{\max} 205 (log ϵ 4.55), 222 (4.60), and 295 (3.72) nm, UV (0.1 N NaOH–MeOH) λ_{\max} 231 (log ϵ 4.60), 303 (3.91), and 374 (3.18) nm; IR (KBr) ν_{\max} 3380, 1720, 1660, and 1510 cm⁻¹; FAB-MS m/z 679 ($M + H$)⁺; HRFAB-MS m/z 679.2729 ($M + H$)⁺, (calcd for C₃₃H₃₉N₆O₁₀ 679.2728). The ¹H and ¹³C NMR data are given in Tables 1 and 2.

TMC-95 D (4): colorless powder; $[\alpha]_D^{23} -36^\circ$ (*c* 0.10, MeOH); R_f value 0.12; UV (MeOH) λ_{\max} 205 (log ϵ 4.47), 221 (4.49), and 301 (3.83) nm, UV (0.1 N HCl–MeOH) λ_{\max} 203 (log ϵ 4.46), 221 (4.48), and 301 (3.82) nm, UV (0.1 N NaOH–MeOH) λ_{\max} 229 (log ϵ 4.47) and 312 (3.89) nm; IR (KBr) ν_{\max} 3400, 1720, 1660, and 1515 cm⁻¹; FAB-MS m/z 679 ($M + H$)⁺; HRFAB-MS m/z 679.2744 ($M + H$)⁺, (calcd for C₃₃H₃₉N₆O₁₀ 679.2728). The ¹H and ¹³C NMR data are given in Tables 1 and 2.

Analyses of Amino Acid and Fatty Acid. TMC-95 A (1.5 mg) was hydrolyzed with 6 N HCl (0.5 mL) at 115 °C for 15 h in a sealed tube. The reaction mixture was extracted with diethyl ether (0.5 mL, twice). The aqueous solution was concentrated and analyzed by chiral TLC (HPTLC plates CHIR, Merck) with a solvent of MeOH–H₂O–CH₃CN (1:1:4), giving a spot of L-aspartic acid (R_f 0.59, cf R_f 0.53 for D-aspartic acid).

The ethereal extracts were concentrated and reacted with (trimethylsilyl)diazomethane, 10% solution in hexane. The resulting mixture was concentrated after standing at room temperature for 0.5 h, and then subjected to GC-MS analysis to give methyl 3-methyl-2-oxopentanoate (**5**) (EI-MS m/z : 144 M⁺, 85, 57).

Sodium Borohydride Reduction, Acid Hydrolysis, and Chiral HPLC Analysis of TMC-95A (1) and -B (2). To a solution of **1** (5.0 mg, 0.007 mmol) in ethanol (1.0 mL) was added sodium borohydride (0.8 mg, 0.021 mmol), and the solution was stirred at ambient temperature for 30 min. The reaction mixture was concentrated to afford a residue which was dissolved in 6 N HCl (0.5 mL), and the mixture was refluxed at 110 °C for 15 h in a sealed tube. The resulting mixture was extracted with CH₂Cl₂ (0.5 mL, twice), and the extracts were dried over anhydrous Na₂SO₄ and concentrated to dryness. The resulting material was analyzed by HPLC to be *d-allo*-2-hydroxy-3-methylvaleric acid (**6a**) and *L*-2-hydroxy-3-methylvaleric acid (**6b**). (Column: CHIRALPAK MA(+), 4.6 mm, i.d. \times 50 mm, Daicel Chemical Industries. Elution: acetonitrile/2 mM aqueous CuSO₄ (1:9). Flow rate: 1.2 mL/min. Detection: UV at 240 nm. Temperature: 37 °C. Retention times of 2-hydroxy-3-methylvaleric acids: *D-allo*-. 19.2 min, *D*-. 22.3 min, *L-allo*-. 29.8 min, *L*-. 36.3 min.)

TMC-95 B (**2**) was treated in the same way to give *D*-2-hydroxy-3-methylvaleric acid (**7a**) and *L-allo*-2-hydroxy-3-methylvaleric acid (**7b**).

Molecular Modeling of 1 and 3. The initial coordinates of **1** and **3** were constructed with standard molecular frag-

ments implemented in SYBYL 6.32 molecular modeling software (Tripos, Inc., St. Louis, MO). Conformational analyses were performed by using Random Search algorithm of Advanced Computation module of SYBYL and Tripos force field. The twelve bonds were allowed to freely rotate during 2000 cycles of random conformational sampling. The resultant structures were exported to QUANTA 4.1 molecular graphics software (Molecular Simulations, Inc., San Diego, CA) and energetically minimized by CHARMm 23.2 force field. To approximate the solvent effect, a distance-dependent dielectric constant was used.

Acknowledgment. We thank Ms. Naoko Fukui for NMR measurements and Ms. Sonoko Shiina for mass measurements.

Supporting Information Available: Copies of ^1H NMR and ^{13}C NMR for TMC-95A–D, and DQF–COSY, ROESY, pfg-HMQC, and pfg-HMBC spectral data for TMC-95A and -C. This material is available free of charge via the Internet at <http://pubs.acs.org>.

JO991375+